

# Study on physicochemical properties of poly(ester-urethane) derived from biodegradable poly( $\epsilon$ -caprolactone) and poly(butylene succinate) as soft segments

Wannarat Panwiriyarat<sup>1</sup> · Varaporn Tanrattanakul<sup>2</sup> ·  
Narong Chueangchayaphan<sup>1</sup>

Received: 21 June 2016 / Revised: 3 October 2016 / Accepted: 16 October 2016 /  
Published online: 21 October 2016  
© Springer-Verlag Berlin Heidelberg 2016

**Abstract** Novel biodegradable polyester-based polyurethanes were developed based on poly( $\epsilon$ -caprolactone) diol (PCL diol) and poly(butylene succinate) diol (PBS diol) as the biodegradable soft segments (SS), and diisocyanate and 1,4-butanediol (BDO) as the hard segment (HS). The PBS diol ( $\overline{M}_n = 2000$  g/mol) was successfully synthesized by melt condensation. The PBS diol and polyurethane sheets were characterized for chemical structure using NMR and FTIR techniques. The effect of hard segments and diisocyanate type on thermo-mechanical properties and hydrolytic degradation were examined by means of tensile testing, TGA, DSC and DMTA. The stress–strain curves of PURs reached the high 715 % elongation at break, 32.5 MPa tensile strength, and 123.8 MPa Young's modulus. Increased hard segment content increased the tensile properties, thermal resistance and  $T_g$ , but the hydrolytic degradation rate decreased. The IPDI-based polyurethane gave lower tensile properties,  $T_g$  and hydrolytic degradation rate, but higher thermal stability than the TDI-based polyurethane.

**Keywords** Polyurethane · Poly( $\epsilon$ -caprolactone) · Poly(butylene succinate) · Biodegradable polymers

---

✉ Wannarat Panwiriyarat  
wannarat.p@psu.ac.th

<sup>1</sup> Faculty of Science and Industrial Technology, Prince of Songkla University, Surat Thani Campus, Surat Thani 84000, Thailand

<sup>2</sup> Department of Materials Science and Technology, Faculty of Science, Prince of Songkla University, Songkhla 90112, Thailand

## Introduction

Environmental issues have currently a high priority in many considerations. For example, increased use of fossil fuels affects the environmental quality, because burning fossil fuels such as coal, natural gas and petroleum oil produces large amounts of carbon dioxide which is one of the greenhouse gases contributing to global warming. In addition, the consumption of traditional petroleum-derived plastics has gradually grown as they are widely utilized, convenient and useful to the human life; but this creates serious problems due to the long lifespan of plastic wastes. The accumulation of petrochemical based commodity plastics waste arises from their nondegradable character and their resistance to microbial degradation. Therefore, to overcome this problem of waste accumulation, plastics with high degree of degradability or biodegradability are desired [1, 2].

Biodegradable polymers have received increasing interest for almost a decade. They have been used in many applications such as packaging, medicine, agriculture and others [3], and they can be categorized into two groups according to origin: natural polymers and synthetic polymers. Naturally biodegradable polymers include polysaccharide (e.g., starch, cellulose), polyesters produced by microorganisms or by plants (e.g., polyhydroxy-alkanoates or PHAs, and poly-3-hydroxybutyrate or PHB), and polyesters synthesized from bio-derived monomers (polylactic acid or PLA). The synthetic biodegradable polymers consist of synthetic polyesters (e.g., polybutylene succinate or PBS, polycaprolactone or PCL, polyglycolic acid or PGA) [3, 4]. Polyesters have potentially hydrolysable ester bonds in their structure. PCL, PHB, PLA and PBS are generally aliphatic polyesters degraded by microorganisms present in the environment [5].

PCL is hydrophobic, semicrystalline and biodegradable aliphatic polyester [2, 6]. It has approximate glass transition temperature  $T_g = -60\text{ }^\circ\text{C}$  and melting temperature  $T_m = 59\text{--}64\text{ }^\circ\text{C}$ , and is applied in food packaging, tissue engineering, dressings for wounds, and drug delivery [3–7]. PCL displays good resistance to water, oil, solvents and chlorine, as well as a very good processing stability [6]. Nevertheless, PCL has some drawbacks including high cost, poor mechanical properties, and low melting temperature, limiting its industrial uses. For example, PCL-based materials are unusable at elevated temperatures [4].

PBS is a highly crystalline polymer, with  $T_g$  around  $-30\text{ }^\circ\text{C}$  and  $T_m$  around  $115\text{ }^\circ\text{C}$  [5, 8]. Its characteristic mechanical properties include good impact strength, thermal resistance, and high flexibility; these are comparable to polypropylene and polyethylene [1, 4, 9, 10]. PBS provides good processability in applications to mulch films, packaging films, bags and flushable hygiene products [4, 8]. PBS is synthesized by polycondensation reaction of 1,4-butanediol (BDO) and succinic acid (SA). These monomers can be derived from both petroleum-based and from bio-based feedstocks [11–16].

Polyurethane (PUR) is a versatile polymeric material used in thermoplastic elastomers, foams, fibers, coatings and adhesives, with a wide range of physico-chemical properties dependent on its chemical composition. The three main components for polyurethane preparation are a diisocyanate, a long chain diol (or

polyol), and a small molecule chain extender. The polyol provides the soft or flexible segments, whereas the reaction between isocyanate and chain extender produces the hard or rigid segments [8, 17, 18]. PUR is typically susceptible to biodegradation under particular conditions due to its hydrolysable backbone. The degradation of polyurethane is dependent on molecular orientation, cross-linking, crystallinity and the chemical groups present. Especially, the polyester-based polyurethanes are readily biodegradable because the degradation rate is governed by the soft segments, where the esters bonds are located [8, 17, 19]. Biodegradable polyesters used in soft segment include PGA, PLA, PCL and PBS [8, 20–22]. Because of its low  $T_g$ , chain cleavage by hydrolysis and nontoxic degradation products, PCL is often used as a compatibilizer or as a soft block in degradable polyurethane formulations [8, 19–31], while PBS has been used as a diol in synthesis of biodegradable polyurethane [14, 31–37].

This research continued the development of segmented PUR which well-defined degradation and mechanical properties. Because the properties of polyurethane depend on its chemical composition, the aim of this study was to develop polyurethane with novel compositions of biodegradable polyols. To the best of our knowledge, there is no prior report on the preparation of poly(ester-urethane) composed of PCL and PBS diols as the soft segments, by solution polymerization.

## Experimental

### Materials

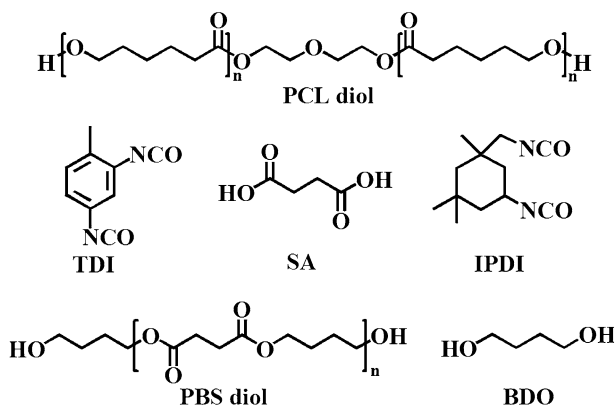
Two commercial PCL diols were used; their molecular weights were 530 g/mol (liquid) and 2000 g/mol (wax). The PCL diols were vacuum dried at 40 °C for 24 h prior to use. PBS diol was synthesized from 1,4-butanediol (BDO) and succinic acid (SA), and its molecular weight of 2000 g/mol (solid). Two types of diisocyanate were employed: isophorone diisocyanate (IPDI), and toluene diisocyanate (TDI). All chemicals used are listed in Table 1, and their chemical structures are shown in Fig. 1. All the chemicals were used as received.

### Synthesis of poly(butylene succinate) diol

Poly(butylene succinate) diol (PBS diol) was prepared through a previously described pathway [31]. PBS diol was synthesized by melt polycondensation from 1.2 mol 1,4-butanediol (BDO) and 1.0 mol succinic acid (SA) at 190°C under nitrogen flow, and the byproduct water was removed by distillation. After reaction for 4 h, 0.1 wt% of tetrabutyl titanate based on the total reactants was added to the reaction flask, and the reaction temperature was raised to 220°C under vacuum (200 mbar) for 1 min, and PBS diol with number average molecular weight ( $\overline{M}_n$ ) of 2000 g/mol, weight average molecular weight ( $\overline{M}_w$ ) of 2940 g/mol, and polydispersity index (PDI) of 1.47 were obtained. Different number average molecular weights ( $\overline{M}_n$ ) were obtained by varying the reaction time, as described in our

**Table 1** List of chemicals

Chemical	Specification	Tradename/producer
1,4-Butanediol	Analytical grade (99.0 %)	Merck
Dibutyl tin dilaurate	Analytical grade (95.0 %)	Aldrich
Isophorone diisocyanate	Analytical grade (98.0 %)	Fluka
Poly( $\epsilon$ -caprolactone) diol	Laboratory grade (two grades: $M_n$ 530 g/mol (liquid) and 2000 g/mol (wax))	Aldrich
Succinic acid	Analytical grade (99.0 %)	Acros
Tetrahydrofuran	Analytical grade (99.8 %)	Fisher Scientific UK Limited
Tetrabutyl titanate	Analytical grade (99.0 %)	Acros
Toluene diisocyanate	Analytical grade (98.0 %)	Fluka

**Fig. 1** Chemical structures of PCL diol, PBS diol, IPDI, TDI, SA and BDO

previous work [31]. Subsequently, the sample was cooled down to room temperature. The obtained product was purified by dissolution in dichloromethane and then precipitation in methanol, to remove low-molecular-weight components as well as traces of the catalyst. The filtered white powder was washed with methanol and dried under vacuum at 40 °C for 24 h. The chemical structure, degree of polymerization ( $\overline{X}_n$ ) and the molecular weight were determined/estimated by  $^1\text{H}$ -NMR,  $^{13}\text{C}$ -NMR, FTIR and size exclusion chromatography (SEC).

### Synthesis of polyurethane (PUR)

Polyurethane was synthesized by solution polymerization, using dichloromethane ( $\text{CH}_2\text{Cl}_2$ ) as solvent, in three-neck round bottom flask equipped with condenser and mechanical stirrer under nitrogen atmosphere. Appropriate amounts of PBS diol, PCL diol, and BDO in  $\text{CH}_2\text{Cl}_2$  (20 w/v %) were put into the reaction flask and stirred until they were completely dissolved. Then, dibutyltin dilaurate (DBTL) was added, followed by diisocyanate. The reaction was carried out at 40 °C for 3 h and

then the mixture was poured into a glass mold and kept overnight at 40 °C in a ventilated oven to obtain a polyurethane sheet after solvent evaporation. The molar ratios IPDI:PBS diol:PCL diol:BDO were varied, as presented in Table 2. Maximally, 0.2 mol of PBS diol was used due to its limited solubility in CH<sub>2</sub>Cl<sub>2</sub>. The PCL diol content varied across molar ratios from 0.80 to 1.0, relative to PBS diol. The hard segment fraction (wt% HS) was calculated from the weight ratio of diisocyanate plus 1,4-butanediol to sum total of all the reactants, including diisocyanate, 1,4-butanediol and the polyols. The contents of hard and soft segments were calculated from Eqs. (1) and (2).

$$\text{Hard segment content (wt\%)} = 100[\text{weight of (isocyanate + 1,4-butanediol)}] / \text{total weight} \quad (1)$$

$$\text{Soft segment content (wt\%)} = 100 \% - \text{Hard segment content (wt\%)} \quad (2)$$

### Material characterization

The structures of the precursors and the polyurethane samples were analyzed using a FTIR spectrometer (BRUKER® EQUINOX 55). Spectra were collected in the range from 400 to 4000 cm<sup>-1</sup>. <sup>1</sup>H and <sup>13</sup>C-NMR spectra were recorded on a BRUKER® AC (400 MHz) Spectrometer. Deuterated chloroform was used as the solvent. A TA Instruments® DSC Q 100 was used in differential scanning calorimetry. The DSC thermograms were recorded with a scan rate of 10 °C/min across the temperature range from –100 to 200 °C under nitrogen atmosphere. Thermogravimetric analysis was carried out on a TA Instruments® TGA Q 500, under nitrogen atmosphere for 30–600 °C range, at a heating rate of 10 °C/min. Approximately 7–10 mg samples were used in all these determinations. A Rheometric Scientific® DMTA V was used to perform dynamic mechanical thermal analysis. The dual-cantilever bending mode was used at a frequency of 1 Hz with strain controlled to 0.01 %, with a heating rate of 3 °C/min across temperature range from –100 to 200 °C. Specimen dimensions

**Table 2** The formula and chemical composition for samples PUR1 to PUR6

Code	Molar ratio				HS (%)	SS (%)
	IPDI	PBS <sub>2000</sub>	PCL <sub>530</sub>	BDO		
PUR1	3.05	0.20	0.80	2.0	51.0	49.0
PUR2	3.05	0.10	0.90	2.0	55.9	44.1
PUR3	3.05	0.05	0.95	2.0	58.7	41.3
PUR4	3.05	–	1.00	2.0	61.8	38.2
					20.5	
PUR5	3.05 (TDI)	0.10	0.90	2.0	51.2	48.8
PUR6	3.05	0.10	0.90 (2000)	2.0	30.0	70.0

were  $10\text{ mm} \times 30\text{ mm} \times 2\text{ mm}$  ( $W \times L \times T$ ). The glass transition temperature ( $T_g$ ) was taken as the location of maximal peak in the  $\tan \delta$  curve. Mechanical tests of the materials were performed on a universal testing machine (Lloyd® LR10 K) at  $25 \pm 2\text{ }^\circ\text{C}$ . A minimum of three test pieces were used in each test and the average values and standard deviations are reported. Young's modulus was determined from the slope of the linear portion in the stress–strain curve. The tensile properties of the polyurethane samples were determined based on ASTM D 412C using a crosshead speed of 500 mm/min. The hardness Shore A (ASTM D2240) was investigated using a Shore Durometer® PTC 408. The hydrolytic degradation of  $10\text{ mm} \times 10\text{ mm} \times 2\text{ mm}$  PUR samples was tested by immersion in a 3 % aqueous NaOH solution at  $37\text{ }^\circ\text{C}$  for various durations, in days. Then, these samples were washed with distilled water and dried in a vacuum oven at  $60\text{ }^\circ\text{C}$  for 3 h. The degree of degradation was determined from the weight loss as follows:

$$\text{Weight loss (\%)} = (W_0 - W_t) \times 100/W_0 \quad (3)$$

where  $W_0$  is the dry weight before degradation and  $W_t$  is the dry weight at time  $t$ .

## Results and discussion

### Synthesis and molecular characterization of PBS diol

To obtain PBS diol, the feed molar ration was set at 1.2 mol BDO per 1.0 mol SA and synthesis by melt condensation used tetrabutyl titanate as catalyst. The molecular structure of PBS diol was determined from  $^1\text{H}$ -NMR and  $^{13}\text{C}$ -NMR spectra (Fig. 2), as well as FTIR technique (Table 3; Fig. 3). The FTIR spectrum of the PBS diol clearly showed the stretching vibrations for  $-\text{OH}$  at  $3442\text{ cm}^{-1}$ , and also confirmed the hydroxyl functional end group represented by absorption peak at  $1046$  and  $653\text{ cm}^{-1}$ . This result is in good agreement with evidence from the NMR. The  $^1\text{H}$ -NMR of PBS diol exhibited signals at 4.12, 3.65, 2.63 and 1.71 ppm, which can be assigned to the methylene protons of  $H_c$ ,  $H_a$ ,  $H_d$  and  $H_b$ , respectively. The intensity at 4.12 ppm is attributable to the methylene protons in the repeating units of PBS diol and the intensity at 3.65 ppm is attributable to the methylene group connected with the terminal hydroxyl group of PBS diol. In addition, the carboxylic acid proton ( $\text{COOH}$ ) cannot be detected. The  $^{13}\text{C}$ -NMR of PBS diol agreed with the results from Zheng et al. [38].  $^{13}\text{C}$ -NMR showed the signal of methylene carbons at 25.22, 29.04 and 64.19 ppm which can be assigned to the methylene carbons of  $C_d$ ,  $C_c$  and  $C_b$ , correspondingly. In addition, the signal of carbonyl carbon ( $C_a$ ) appeared at the chemical shift of 172.30 ppm. These data indicate that PBS diol was successfully prepared, and it was used as a precursor in synthesizing polyurethane.

### Preparation of polyurethanes

Colorless, soft and transparent polyurethane sheets were obtained by solution polymerization. The FTIR assignments to precursors and to polyurethane are listed

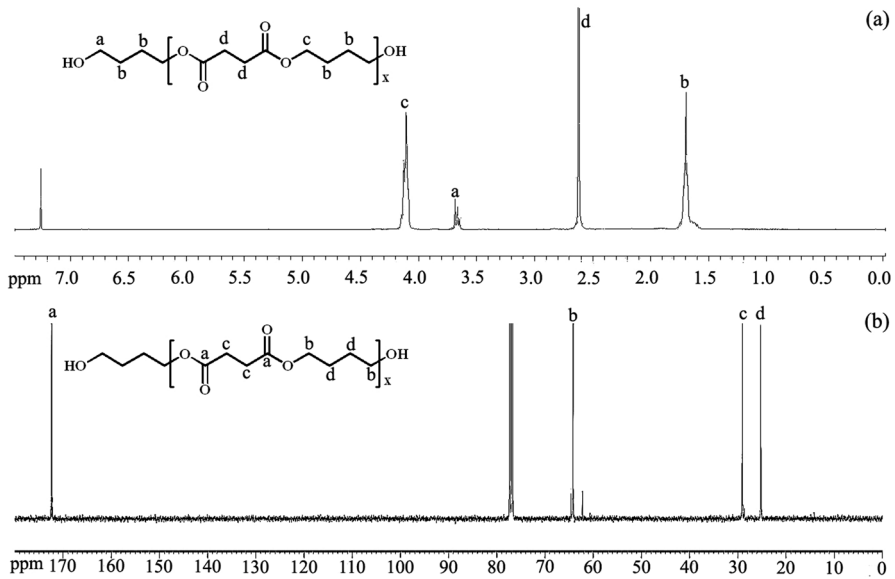


**Fig. 2** a  $^1\text{H}$ -NMR of PBS diol and b  $^{13}\text{C}$ -NMR of PBS diol

in Table 3. The diisocyanate (in IPDI and TDI) had its main unique peaks at 2258 and  $2260\text{ cm}^{-1}$ , related to the unreacted  $-\text{N}=\text{C}=\text{O}$  groups. The PCL diol and PBS diol exhibited as main peaks those from the stretching vibrations of  $-\text{OH}$  at  $3440\text{--}3430\text{ cm}^{-1}$ , the stretching vibrations of  $-\text{C}=\text{O}$  at  $1731\text{--}1718\text{ cm}^{-1}$ , and the  $-\text{C}-\text{O}-\text{C}$  stretching vibrations at  $1167\text{--}1165\text{ cm}^{-1}$ . The synthesis of polyurethane was successful: it was confirmed by FTIR as has been done in many prior publications [19, 20, 22, 24, 25, 31]. The free  $-\text{N}=\text{C}=\text{O}$  of diisocyanate reacted with the  $-\text{OH}$  groups of diols and the chain extender, causing absence of the  $-\text{N}=\text{C}=\text{O}$  and  $-\text{OH}$  absorbance peaks in the PUR spectra of Fig. 3. This indicates that chemical reactions between diisocyanate groups and hydroxyl end groups of diols and chain extender took place, forming polyurethane linkages. In addition, new absorption peaks of free  $-\text{N}-\text{H}$  and the hydrogen bonds of  $-\text{N}-\text{H}$  groups emerged, as a small shoulder near  $\sim 3500$  and at  $3325\text{ cm}^{-1}$ , respectively. The absorption peak of  $-\text{C}=\text{O}$  shifted to a lower value at  $1692\text{ cm}^{-1}$ , indicating the  $-\text{C}=\text{O}$  hydrogen bonds stretching in the urethane linkages. The  $-\text{CHN}$  vibrations of associated secondary urethane groups emerged at  $1529\text{ cm}^{-1}$ , and  $-\text{C}-\text{O}$  stretching vibrations at  $1235\text{ cm}^{-1}$ .

### Mechanical properties of polyurethanes

Figure 4 exhibits the tensile stress–strain curves for polyurethane samples, and the corresponding tensile characteristics are listed in Table 4. The mechanical properties of polyurethane involve several factors, such as the crystallinity of the soft segments, the crosslink density and the hard segment content [19, 39]. It was observed that PUR2-PUR5 exhibited the yielding and plastic deformation behavior,

**Table 3** Assignment of FTIR peaks to groups in the chemical structures of the reactants and of polyurethane

	Assignment	Wavenumber (cm <sup>-1</sup> )
IPDI	$\nu$ (CH <sub>2</sub> )	2956
	$\nu$ (N=C=O)	2260
	$\delta$ (CH <sub>2</sub> )	1463
	$\nu$ C(CH <sub>3</sub> ) <sub>2</sub> of carbocyclic ring	1366
TDI	$\nu$ (N=C=O)	2258
	Overtone of aromatic substitution	1781, 1721
	$\nu$ (C=C) in aromatic compound	1600–1500
	$\delta$ (C=C–H)	890–815
PCL diol	$\nu$ (O–H)	3442
	$\nu$ (C=O)	1731
	$\nu$ (C–O–C)	1167
PBS diol	$\nu$ (O–H)	3430
	$\nu$ (C=O)	1718
	$\nu$ (C–O–C)	1165
	$\nu$ (C–O) in primary alcohol	1046
PUR	$\delta$ (C–O–H)	653
	$\nu$ (N–H)	~ 3500
	$\nu$ (N–H) H-bonded	3325
	$\nu$ (C=O) H-bonded	1692
	$\delta$ (N–H) + $\nu$ (C–N)	1529
	Amide III + $\nu$ (C–O)	1235

while PUR1 and PUR6 showed soft and weak behavior. The increased PBS diol content and molecular weight of PCL diol in PUR1 and PUR6 led to a decrease in hard segment content which attributed to the weaker hydrogen bonding between the hard segment and soft segment, therefore PUR1 and PUR6 had more reduced in mechanical properties. The incorporation of PCL diol in the polyester-based polyurethane can be assessed from cases PUR1 to PUR4, in which the PBS diol:PCL diol molar ratio varies from 0.2:0.8 to 0:1.0, at constant 3.05:2.0 IPDI:BDO molar ratio. The molecular weights of the PCL diol and the PBS diol were 530 g/mol and 2000 g/mol, respectively. With increasing PCL diol content or hard segment content, the tensile strength and elongation at break tend to increase, but their Young's modulus were not different. According to Tsou et al. [20] and Han et al. [30], the polyurethane with higher hard segment content had a higher elongation at break than the lower one. This explains that aggregation of hard segment domain by hydrogen-bonded interaction supports the formation of microphase separation. This hard segment domain provides a physical crosslinked network structure between linear polyurethane chains, so that the polyurethane has the elastomeric properties. Furthermore, the effects of molecular weight of PCL diol on the tensile properties of polyurethane can be assessed from PUR2 and PUR6. The molecular weight of the precursors also relates to the hard segment content. It is



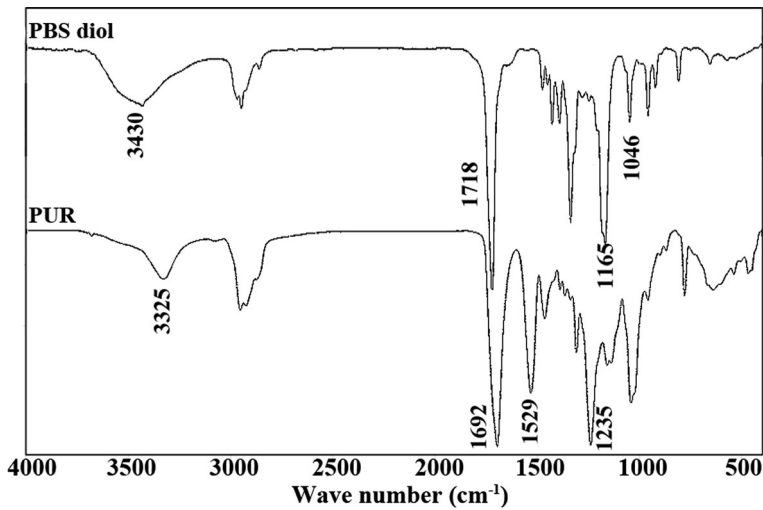


**Fig. 3** FTIR spectra of PBS diol and polyurethane

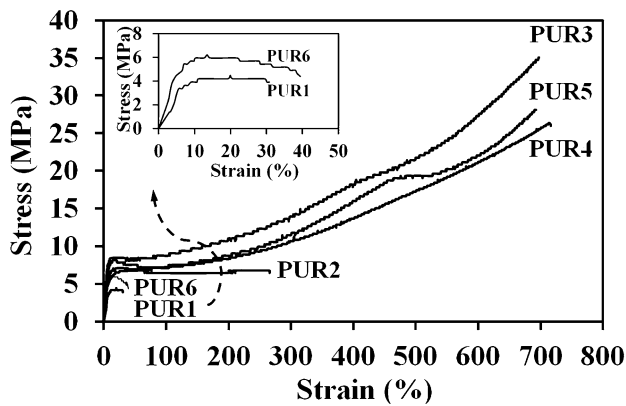


**Fig. 4** Stress-strain curves of PUR1-PUR6

**Table 4** Tensile characteristics of PUR1-PUR6

Code	Young's modulus (MPa)	Tensile strength (MPa)	Elongation at break (%)
PUR1	94.3 ± 26.3	3.7 ± 0.4	30 ± 1
PUR2	100.2 ± 22.5	6.8 ± 0.9	275 ± 29
PUR3	115.4 ± 14.6	35.2 ± 0.9	680 ± 35
PUR4	110.5 ± 12.8	27.9 ± 2.8	710 ± 19
PUR5	123.8 ± 5.9	25.8 ± 2.2	715 ± 44
PUR6	101.2 ± 0.7	3.3 ± 0.4	32 ± 11

observed that PUR6 with 2000 g/mol PCL diol exhibited lower tensile strength and elongation at break than the corresponding PUR2 with 530 g/mol PCL diol. The hard segment content of PUR6 was only 30.0 % while PUR2 has 55.9 % which significantly affects the mechanical properties. Increasing the hard segment content contributes to microphase separation, which can improve the mechanical properties [20, 39, 40]. At a specified molecular weight of PCL diols and NCO:OH molar ratio, the influence of the diisocyanate type on the tensile properties was assessed as follows. Two diisocyanates with asymmetric molecular architectures were employed: a cycloalkane diisocyanate (IPDI) and an aromatic diisocyanate (TDI), in PUR2 and PUR5, respectively. According to Prisacariu [41], the structural rigidity of aromatic hard segments normally provides polyurethane elastomers with high tensile strength and modulus. This phenomenon was also observed in this study. The tensile behaviors of PUR2 and PUR5 were overall similar, but the TDI-based PUR case PUR5 showed higher tensile strength and elongation at break than the IPDI-based PUR PUR2. This implies that the molecular structure of diisocyanate influenced the mechanical properties of the polyurethanes.

### Thermal properties of polyurethanes

The thermal behavior of the PURs was examined by TGA, DSC and DMTA. Figure 5 presents the TGA curves of diol precursors (BDO, PCL<sub>530</sub>, PCL<sub>2000</sub> and PBS<sub>2000</sub>), and those of the PURs are in Fig. 6. The onset decomposition temperature ( $T_{\text{onset}}$ ) and the decomposition temperature peak ( $T_{\text{peak}}$ ) are listed in Table 5. It was found that BDO and PCL<sub>2000</sub> exhibited the lowest and the highest thermal degradation temperature, respectively, whereas PCL<sub>530</sub> and PBS<sub>2000</sub> had similar thermal degradation temperatures. It can be assumed that the thermal stability of precursors depends on their molecular weight and chemical structure. The effects of PCL diols content or hard segment content on the thermal stability was studied from PUR1–PUR4. On increasing PCL diol content or hard segment content, the thermal stability improved. This agrees well with the study of Tsou et al. [20], which showed an increasing decomposition temperature, or improved thermal resistance,

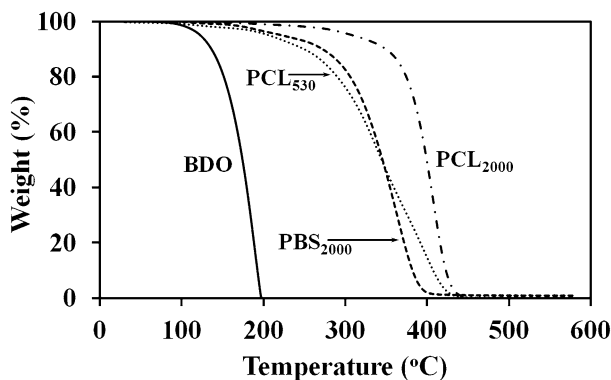
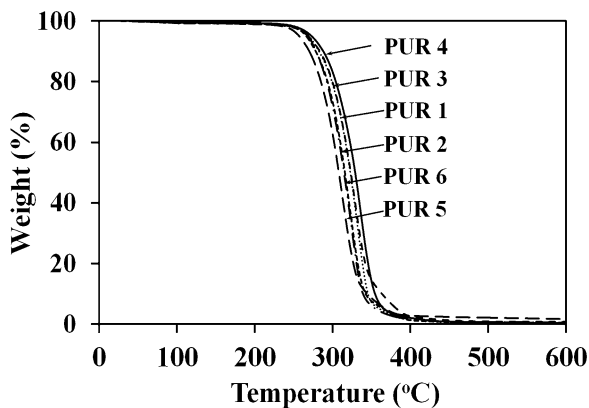


Fig. 5 Thermogravimetric response curves for the diols and the chain extender

**Fig. 6** Thermogravimetric response curves for PUR1–PUR6**Table 5** Thermal decomposition characteristics of PUR1–PUR6

Code	TGA		DSC	DMTA
	$T_{\text{onset}}$ (°C)	$T_{\text{peak}}$ (°C)	$T_g$ (°C)	$T_g$ (°C)
PUR1	296	325	1.3	32.5/76
PUR2	290	320	14.8	48.9/83
PUR3	299	330	24.3	49.6/100
PUR4	301	335	35.2	55.7/104
PUR5	279	315	17.2	43.0/68
PUR6	291	325	−52.0	6.5/53

for polyurethane as its hard segment content increased. Additionally, an increase in the PCL diol chain length slightly improved thermal stability further, so that PUR6 had better thermal stability than PUR2: the PCL<sub>2000</sub> precursor provided better thermal stability than the PCL<sub>530</sub>, as shown in Fig. 5. Concerning the effects of diisocyanate type, the TDI hard segments had slightly lower thermal degradation temperature than the IPDI-based ones, as shown in our previous work [25]. As a result, PUR5 had poorer thermal stability than PUR2. In summary, the synthesis method, the raw materials used, the hard segment and soft segment contents, all influenced the thermal stability of polyurethane.

The microphase separation and phase mixing in polyurethane can be estimated from the glass transition temperature, observed by DSC or DMTA techniques. The DSC thermograms obtained with the second heating scan of the diol precursors and the PURs are shown in Figs. 7 and 8, respectively. The diol precursors were semi-crystalline prepolymers. PCL<sub>530</sub>, PCL<sub>2000</sub> and PBS<sub>2000</sub> had double melting peaks ( $T_m$ ) at −9/15 °C, 44/49 °C and 95/107 °C, respectively. All the PURs showed only one  $T_g$  and did not exhibit any crystallization or melting peaks, during either cooling or heating, except PUR6 which showed the recrystallization temperature peak and the melting temperature peak at 21.7 and 43.1 °C, respectively. Undoubtedly, PUR1–PUR5 were amorphous polymer while PUR6 was semi-crystalline polymer. This indicates that no phase separation of the soft and the hard segments occurred in

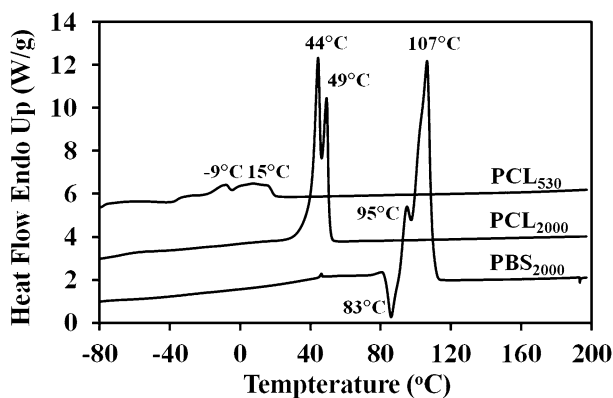


**Fig. 7** Differential scanning calorimetry responses during the second heating of diol precursors

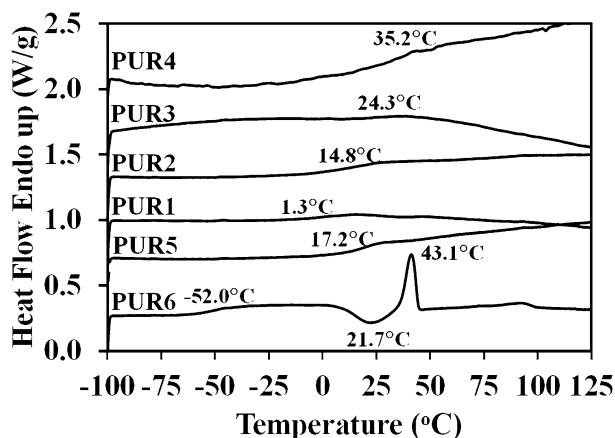


**Fig. 8** Differential scanning calorimetry responses during the second heating of PUR1-PUR6

the obtained polyurethanes which were observed by DSC. From our previous study [25], the TDI-based hard segment and the IPDI-based hard segment had high  $T_g$  values, at 107 and 109 °C, respectively. The  $T_g$  increased with PCL diol (or hard segment) content. This suggests that hydrogen bonding of the matrix increased with the hard segment content, which reduced the molecular mobility in the structure. However,  $T_g$  decreased with PCL diol chain length resulting in the lowest  $T_g$  of PUR6. The  $T_g$  decreased with increasing soft segment molecular weight because the free volume and mobility of macromolecules increased which was caused by the lower content of hard segment in this PUR6. When the IPDI-based polyurethane (PUR2) is compared with the TDI-based polyurethane (PUR5), the latter had the higher  $T_g$ . This indicates that the rigid aromatic ring in TDI hindered molecular mobility.

Figures 9 and 10 show the temperature dependence of storage modulus and of  $\tan \delta$  for the PURs. Glass transition temperature ( $T_g$ ) was determined from the peak

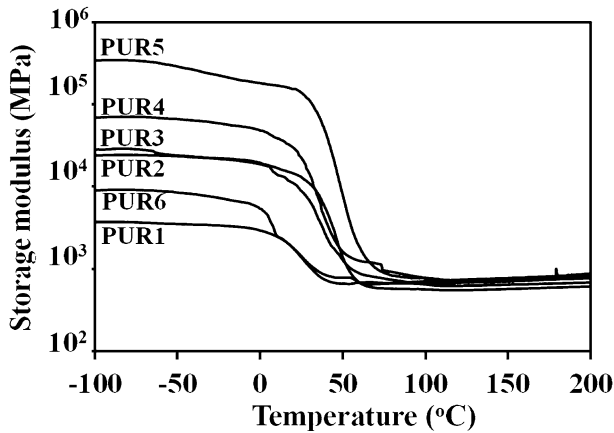
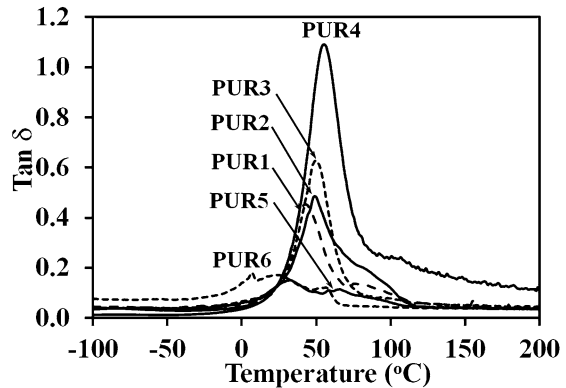


**Fig. 9** Storage modulus vs. temperature for PUR1-PUR6

**Fig. 10** Tan delta vs. temperature for PUR1-PUR6



magnitude of  $\tan \delta$  curve. The  $\tan \delta$  curves show one main and one shoulder peaks for PUR1, PUR2, PUR3, and PUR4 and two peaks for PUR5 and PUR6. These two peaks indicate phase separation. The effects of variable hard segment content can be assessed from PUR1 to PUR4. The data show that both  $E'$  and peak magnitude of  $\tan \delta$  tended to increase with hard segment content. The storage modulus at the glassy state had the same rank order as the Young's modulus (listed in Table 5), across all PUR samples, and increased with the hard segment content. The molecular motion of the soft segment was probably restricted by hard microcrystalline domains, so increasing hard segment content increased the  $T_g$ . Similarly, the storage modulus of PUR5 was greater than that of PUR2. The aromatic diisocyanate provided larger storage modulus to polyurethane than the aliphatic diisocyanate, due to the rigidity of aromatic ring [41]. Concerning the influence of PCL chain length (comparing PUR2 and PUR6), increasing the soft segment chain length reduced the storage modulus and  $T_g$  in PUR6 as the molecular mobility was facilitated.

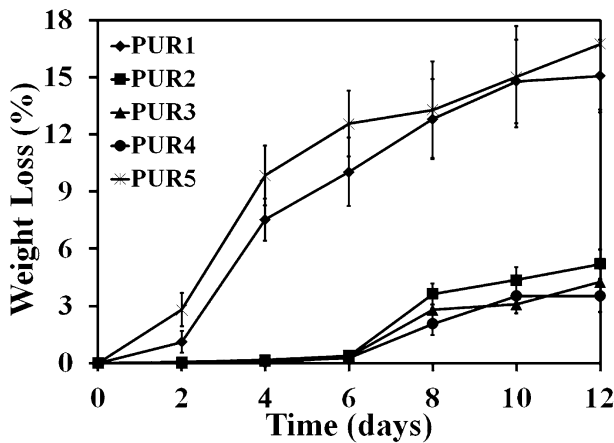


**Fig. 11** Hydrolytic degradation of PUR1-PUR5

Based on the DSC and the DMTA results, the different type and condition of the measurement techniques (DSC and DMTA) affect on the detection and  $T_g$  of polymers. DMTA seems to be more sensitive than DSC to detect thermal transitions of polyurethane. Phase separation of the soft and the hard segments was clearly visible in the DMTA experiments.

### Degradation study

The hydrolytic degradation in NaOH solution at 37 °C for PUR1 to PUR5 is shown in Fig. 11. The PUR6 case could not be weighed because it broke into small pieces during testing. The weight loss by hydrolytic degradation with test time, and increasing the PCL diol content (or hard segment content) reduced the degradation rate, on comparing PUR1 to PUR4. The hard segments acted as physical crosslinks in the polyurethane structure, so the hard segment content resisted decomposition. In addition, PUR5 exhibited faster hydrolytic degradation than PUR2, because the aromatic diisocyanate provides not only more rigid but also higher hydrolytic degradation than the aliphatic one to polyurethane [42].

### Conclusions

PBS diol was successfully synthesized as a diol precursor for polyurethane preparation, and its chemical structure was confirmed by FTIR,  $^1\text{H-NMR}$  and  $^{13}\text{C-NMR}$ . Polyurethanes with novel composition were also successfully prepared with biodegradable PCL diol or PBS diol as soft segments by solution polymerization, with IPDI or TDI and BDO acting as hard segments. FTIR was used to determine the urethane linkage formation. The effects of PCL diol:PBS diol ratio, type of diisocyanate, and molecular weight of PCL diol on the mechanical and thermal properties as well as on hydrolytic degradation were investigated. Generally, the

PURs exhibited plastic deformation, except for the cases PUR1 and PUR6 that showed weak and soft deformation behavior. The tensile properties, thermal stability and glass transition temperature increased, but the hydrolytic degradation rate decreased with the hard segment content. The TDI-based polyurethanes had higher tensile properties,  $T_g$  and hydrolytic degradation rate, but lower thermal stability than IPDI-based polyurethanes.

**Acknowledgments** This research was financially supported by the Higher Education Research Promotion and National Research University Project of Thailand, Office of the Higher Education Commission (SIT580645S) and by Prince of Songkla University, Surat Thani Campus, 2015. The authors would like to express their gratitude to the Faculty of Science and Industrial Technology, Prince of Songkla University, Surat Thani Campus. We also thank Assoc. Prof. Dr. Seppo Karrila for assistance with manuscript preparation.

## References

1. Tokiwa Y, Clabia BP, Ugwu CU, Aiba S (2009) Review biodegradability of plastic. *Int J Mol Sci*. doi:[10.3390/ijms10093722](https://doi.org/10.3390/ijms10093722)
2. Chiellini E, Solaro R (2003) Biodegradable polymer and plastics. New York, USA
3. Platt DK (2006) Biodegradable polymers: market report. Shropshire, UK
4. Smith R (2005) Biodegradable polymers for industrial applications. Cambridge, UK
5. Bastioli C (2014) Handbook of biodegradable polymers, 2nd edn. Shropshire, UK
6. Woodruff MA, Hutmacher DW (2010) The return of a forgotten polymer-polycaprolactone in the 21st century. *Prog Polym Sci* 35:1217–1256. doi:[10.1016/j.progpolymsci.2010.04.002](https://doi.org/10.1016/j.progpolymsci.2010.04.002)
7. Liu JY, Reni L, Wei Q, Wu JL, Liu S, Wang YJ, Li GY (2011) Fabrication and characterization of polycaprolactone/calcium sulfate whisker composites. *E-Xpress Polym Lett* 5(8):742–752. doi:[10.3144/expresspolymlett.2011.72](https://doi.org/10.3144/expresspolymlett.2011.72)
8. Vroman I, Tighzert L (2009) Review biodegradable polymers. *Materials* 2:307–344. doi:[10.3390/ma2020307](https://doi.org/10.3390/ma2020307)
9. Chen RY, Zou W, Wu CR, Jia SK, Huang Z, Zhang GZ, Yang ZT, Qu JP (2014) Poly(lactic acid)/poly(butylene succinate)/calcium sulfate whiskers biodegradable blends prepared by vane extruder: analysis of mechanical properties, morphology, and crystallization behavior. *Polym Test* 34:1–9. doi:[10.1016/j.polymertesting.2013.12.009](https://doi.org/10.1016/j.polymertesting.2013.12.009)
10. Dorez G, Taguet A, Ferry L, Cuesta JML (2014) Phosphorous compounds as flame retardants for polybutylene succinate/flax biocomposite: additive versus reactive route. *Polym Degrad Stabil* 102:152–159. doi:[10.1016/j.polymdegradstab.2014.01.018](https://doi.org/10.1016/j.polymdegradstab.2014.01.018)
11. Phua YJ, Chow WS, Mohd Ishak ZA (2011) The hydrolytic effect of moisture and hygrothermal aging on poly(butylenes succinate)/organo-montmorillonite nanocomposites. *Polym Degrad Stabil* 96(7):1194–1203. doi:[10.1016/j.polymdegradstab.2011.04.017](https://doi.org/10.1016/j.polymdegradstab.2011.04.017)
12. Ravati S, Favis BD (2013) Tunable morphologies for ternary blends with poly(butylene succinate): partial and complete wetting phenomenon. *Polymer* 54(13):3271–3281. doi:[10.1016/j.polymer.2013.04.005](https://doi.org/10.1016/j.polymer.2013.04.005)
13. Khalil F, Galland S, Cottaz A, Joly C, Degraeve P (2014) Polybutylene succinate adipate/starch blends: a morphological study for the design of controlled release films. *Carbohydr Polym* 108:272–280. doi:[10.1016/j.carbpol.2014.02.062](https://doi.org/10.1016/j.carbpol.2014.02.062)
14. Sonnenschein MF, Guillaudeu SJ, Landes BG, Wendt BL (2010) Comparison of adipate and succinate polyesters in thermoplastic polyurethanes. *Polymer* 51:3685–3692. doi:[10.1016/j.polymer.2010.06.012](https://doi.org/10.1016/j.polymer.2010.06.012)
15. Jbilou F, Joly C, Galland S, Belard L, Desjardin V, Bayard R, Dole P, Degraeve P (2013) Biodegradation study of plasticized corn flour/poly(butylene succinate-co-butylene adipate) blends. *Polym Test* 32:1565–1575. doi:[10.1016/j.polymertesting.2013.10.006](https://doi.org/10.1016/j.polymertesting.2013.10.006)
16. Díaz A, Katsarava R, Puiggali J (2014) Review synthesis, properties and applications of biodegradable polymers derived from diols and dicarboxylic acids: from polyesters to poly(ester amide)s. *Int J Mol Sci* 15:7064–7123. doi:[10.3390/ijms15057064](https://doi.org/10.3390/ijms15057064)

17. Howard GT (2002) Biodegradation of polyurethane: a review. *Int Biodeter Biodegr* 49:245–252. doi:[10.1016/S0964-8305\(02\)00051-3](https://doi.org/10.1016/S0964-8305(02)00051-3)
18. Treviño AL, Sánchez GG, Herrera RR, Aguilar CN (2012) Microbial enzymes involved in polyurethane biodegradation: a review. *J Polym Environ* 20:258–265. doi:[10.1007/s10924-011-0390-5](https://doi.org/10.1007/s10924-011-0390-5)
19. Barriani BR, Maria de Carvalho S, Oréfice RL, Rocha de Oliveira AA, Pereira MM (2015) Synthesis and characterization of biodegradable polyurethane films based on HDI with hydrolyzable cross-linked bonds and a homogeneous structure for biomedical applications. *Mat Sci Eng C* 52:22–30. doi:[10.1016/j.msec.2015.03.027](https://doi.org/10.1016/j.msec.2015.03.027)
20. Tsou CH, Lee HT, Tsai HA, Cheng HJ, Suen MC (2013) Synthesis and properties of biodegradable polycaprolactone/polyurethanes by using 2,6-pyridinedimethanol as a chain extender. *Polym Degrad Stab* 98:643–650. doi:[10.1016/j.polymdegradstab.2012.11.010](https://doi.org/10.1016/j.polymdegradstab.2012.11.010)
21. Domanska A, Boczkowska A (2014) Biodegradable polyurethanes from crystalline prepolymers. *Polym Degrad Stab* 108:175–181. doi:[10.1016/j.polymdegradstab.2014.06.017](https://doi.org/10.1016/j.polymdegradstab.2014.06.017)
22. Arcana IM, Bundjali B, Hasan M, Hariyawati K, Mariani H, Anggraini SD, Ardana A (2010) Study on properties of poly(urethane-ester) synthesized from prepolymers of  $\epsilon$ -caprolactone and 2,2-dimethyl-1,3-propanediol monomers and their biodegradability. *J Polym Environ* 18:188–195. doi:[10.1007/s10924-010-0189-9](https://doi.org/10.1007/s10924-010-0189-9)
23. Maafi EM, Malek F, Tighzert L, Dony F (2010) Synthesis of polyurethane and characterization of its composites based on Alfa cellulose fibers. *J Polym Environ* 18:638–646. doi:[10.1007/s10924-010-0218-8](https://doi.org/10.1007/s10924-010-0218-8)
24. Panwiriayat W, Tanrattanakul V, Pilard JF, Pasetto P, Khaokong C (2013) Preparation and properties of bio-based polyurethane containing polycaprolactone and natural rubber. *J Polym Environ* 21:807–815. doi:[10.1007/s10924-012-0567-6](https://doi.org/10.1007/s10924-012-0567-6)
25. Panwiriayat W, Tanrattanakul V, Pilard JF, Pasetto P, Khaokong C (2013) Effect of the diisocyanate structure and the molecular weight of diols on bio-based polyurethanes. *J Appl Polym Sci* 130(1):453–462. doi:[10.1002/app.39170](https://doi.org/10.1002/app.39170)
26. Valério A, Conti DS, Araújo PHH, Sayer C, Rocha SRP (2015) Synthesis of PEG-PCL-based polyurethane nanoparticles by miniemulsion polymerization. *Colloid Surface B* 135:35–41. doi:[10.1016/j.colsurfb.2015.07.044](https://doi.org/10.1016/j.colsurfb.2015.07.044)
27. Chan LHC, Correa RS, Coronado RFV, Uc JMC, Rodríguez JVC, Quintana P, Pérez PB (2010) Degradation studies on segmented polyurethanes prepared with HMDI, PCL and different chain extenders. *Acta Biomater* 6:2035–2044. doi:[10.1016/j.actbio.2009.12.010](https://doi.org/10.1016/j.actbio.2009.12.010)
28. Hernández LM, Sánchez FH, Ribelles JLG, Serra RS (2011) Segmented poly(urethane-urea) elastomers based on polycaprolactone: structure and properties. *Appl Polym Sci* 119:2093–2104. doi:[10.1002/app.32929](https://doi.org/10.1002/app.32929)
29. Wu CL, Chiu SH, Lee HT, Suen MC (2015) Synthesis and properties of biodegradable polycaprolactone/polyurethanes using fluoro chain extenders. *Polym Adv Technol*. doi:[10.1002/pat.3737](https://doi.org/10.1002/pat.3737)
30. Han J, Chen B, Ye L, Zhang A, Zhang J, Feng Z (2009) Synthesis and characterization of biodegradable polyurethane based on poly( $\epsilon$ -caprolactone) and L-lysine ethyl ester diisocyanate. *Front Mater Sci China* 3(1):25–32. doi:[10.1007/s11706-009-0013-4](https://doi.org/10.1007/s11706-009-0013-4)
31. Panwiriayat W, Tanrattanakul V, Pilard JF, Burel F, Kébir N (2016) Elaboration and properties of renewable polyurethanes based on natural rubber and biodegradable poly(butylene succinate) soft segments. *J Appl Polym Sci* 42943:1–8. doi:[10.1002/APP.42943](https://doi.org/10.1002/APP.42943)
32. Oh HJ, Kim WY, Lee DS, Lee YS (2000) Polyurethane anionomers based on poly(butylene succinate), 4,4'-methylenebis(phenyl isocyanate), and 2,2-bis(hydroxymethyl)propionic acid. *J Ind Eng Chem* 6(6):425–430
33. Lee SI, Yu SC, Lee YS (2001) Degradable polyurethanes containing poly(butylene succinate) and poly(ethylene glycol). *Polym Degrad Stab* 72:81–87. doi:[10.1016/S0141-3910\(00\)00205-6](https://doi.org/10.1016/S0141-3910(00)00205-6)
34. Zeng JB, Li YD, Zhu QY, Yang KK, Wang XL, Wang YZ (2009) A novel biodegradable multiblock poly(ester urethane) containing poly(L-lactic acid) and poly(butylene succinate) blocks. *Polymer* 50:1178–1186. doi:[10.1016/j.polymer.2009.01.001](https://doi.org/10.1016/j.polymer.2009.01.001)
35. Moon SY, Park YD, Kim CJ, Won CH, Lee YS (2003) Effect of chain extenders on polyurethane containing both poly(butylene succinate) and poly(ethylene glycol) as soft segments. *Bull Korean Chem Soc* 24(9):1361–1364
36. Poussard L, Mecheri A, Mariage J, Batakat I, Bonnaud L, Raquez JM, Dubois P (2014) Synthesis of oligo(butylene succinate)-based polyurethanes. *J Renew Mater* 1(10):13–22. doi:[10.7569/JRM.2013.634132](https://doi.org/10.7569/JRM.2013.634132)



37. Lu X, Huang J, He G, Yang L, Zhang N, Zhao Y, Qu J (2013) Preparation and characterization of cross-linked poly(butylene succinate) by multifunctional toluene diisocyanate-trimethylolpropane polyurethane prepolymer. *Ind Eng Chem Res* 52:13677–13684. doi:[10.1021/ie4020342](https://doi.org/10.1021/ie4020342)
38. Zheng L, Li C, Zhang D, Guan G, Xiao Y, Wang D (2011) Synthesis, characterization and properties of novel biodegradable multiblock copolymers comprising poly(butylene succinate) and poly(1,2-propylene terephthalate) with hexamethylene diisocyanate as a chain extender. *Polym Int* 60:666–675. doi:[10.1002/pi.3000](https://doi.org/10.1002/pi.3000)
39. Alishiri M, Shojaei A, Abdekhodie MJ, Yeraneh H (2014) Synthesis and characterization of biodegradable acrylated polyurethane based on poly( $\epsilon$ -caprolactone) and 1,6-hexamethylene diisocyanate. *Mater Sci Eng, C* 42:763–773. doi:[10.1016/j.msec.2014.05.056](https://doi.org/10.1016/j.msec.2014.05.056)
40. Tsou CH, Lee HT, Guzman MD, Tsai HA, Wang PN, Cheng HJ, Suen MC (2015) Synthesis of biodegradable polycaprolactone/polyurethane by curing with H<sub>2</sub>O. *Poym Bull* 72:1545–1561. doi:[10.1007/s00289-015-1356-x](https://doi.org/10.1007/s00289-015-1356-x)
41. Prisacariu C (2011) *Polyurethane elastomer from morphology to mechanical aspects*. New York, USA
42. Pignatello R (2013) *Advances in biomaterials science and biomedical applications*. doi:[10.5772/56420](https://doi.org/10.5772/56420)